Magnetic resonance diffusion tensor imaging-based evaluation of optic-radiation shape and position in meningioma☆

Xueming Lv, Xiaolei Chen, Bainan Xu, Jiashu Zhang, Gang Zheng, Jinjiang Li, Fangye Li, Guochen Sun

Department of Neurosurgery, Chinese PLA General Hospital, Chinese PLA Postgraduate Medical School, Beijing 100853, China

Abstract

Employing magnetic resonance diffusion tensor imaging, three-dimensional white-matter imaging and conventional magnetic resonance imaging can demonstrate the tumor parenchyma, peritumoral edema and compression on surrounding brain tissue. A color-coded tensor map and three-dimensional tracer diagram were applied to clearly display the optic-radiation location, course and damage. Results showed that the altered anisotropy values of meningioma patients corresponded with optic-radiation shape, size and position on both sides. Experimental findings indicate that the magnetic resonance diffusion tensor imaging technique is a means of tracing and clearly visualizing the optic radiation.
Key Words: magnetic resonance; diffusion tensor imaging; diffusion tensor tractography; meningioma; optic radiation
Abbreviations: MRI, magnetic resonance image; DTI, diffusion tensor imaging; FA, fractional anisotropy

Xueming Lv☆, Studying for doctorate, Associate chief physician, Department of Neurosurgery, Chinese PLA General Hospital, Chinese PLA Postgraduate Medical School, Beijing 100853, China

Xueming Lv and Xiaolei Chen contributed equally to this work.

Corresponding author: Bainan Xu, M.D., Chief physician, Department of Neurosurgery, Chinese PLA General Hospital, Chinese PLA Postgraduate Medical School, Beijing 100853, China
sjwk301@Gmail.com

INTRODUCTION

The optic radiation, composed of axons elicited from lateral geniculate neurons in the thalamus, can transmit visual information to the occipital visual cortex and clearly describe the optic-radiation course *in vivo*, and its structure and function are hot spots in neurosurgery research. The Klingler method for white-matter fiber anatomy can clarify the morphological characteristics of the optic radiation and comprehensively introduce a complex relationship among fiber bundles[1-5]. The optic radiation can be infiltrated or damaged in brain lesions, and can also be impaired when extracerebral tumors grow beside the optic radiation.
Diffusion tensor imaging (DTI) and fiber tractography can visualize white-matter fiber and further improve the understanding of fiber bundles *in vivo*, and these means have been widely used to study white-matter architecture and the integrity of the normal and affected brain. The three-dimensional white-matter fiber model is determined by the main direction of diffusion in the adjacent voxel space. So far, DTI is the only noninvasive means of visualizing the shift, displacement and destruction of white-matter tracts[6-10]. There is strong evidence that DTI can reconstruct white-matter fiber in the brain[11-21].

The main principle of nerve tumor surgery is not only to maximize the removal of tumor tissue but also to minimize the damage to normal nerve function during surgery, such as damage to white-matter fiber bundles. Although an extracerebral tumor does not invade the cerebral cortex and/or white matter, caution should be taken to clarify the correlation between the tumor and peritumoral tissue, as well as the effect on adjacent white-matter fibers. Conventional magnetic resonance imaging (MRI) accurately displays tumor localization but cannot clearly investigate the tumor occupation of white-matter fiber bundles. For example, a strong peritumoral signal in T2-weighted sequences and fluid attenuated inversion recovery sequences has a variety of manifestations, including tumor cell proliferation in malignant meningiomas and white-matter edema, which are important indicators for the judgment of white-matter fiber tracts. Other methods such as conventional functional MRI, positron emission computer tomography and magnetoencephalography can record and evaluate cerebral cortex function[22-23]. However, there has been little progress in the assessment of white-matter injury. Magnetic resonance (MR)-DTI clearly displays the morphology and structure of white matter, and is considered the only noninvasive way to visualize white matter

in vivo.

In this study, DTI-based three-dimensional tracing of white matter was employed to noninvasively visualize a meningioma and surrounding white matter *in vivo*, display the optic-radiation course, reflect the optic-radiation pathology and its anatomical relationship with an adjacent tumor, and clarify the effect of acute or chronic extracerebral occupying lesions on white-matter fiber bundles.

RESULTS

Quantitative analysis of subjects
Eighteen meningioma patients underwent MR-DTI examination within 3 days of conventional surgical treatment. Preoperative tumor apoplexy or hernia formation was not observed. All 18 patients entered the final analysis with no loss.

Baseline information for meningioma patients (Table 1)

Table 1   Clinical information on meningioma patients

Case	Gender	Age (year)	Meningioma type	Lesion	Duration of disease (year)
1	Female	47	Benign	Right vertex and occiput, lateral visual reflex	5
2	Female	65	Benign	Right sphenoidal crest, rostral visual reflex	2
3	Male	60	Malignant	Trigone of left ventricle, caudal visual reflex	2.5
4	Male	59	Benign	Right vertex and occiput, caudal visual reflex	4
5	Male	48	Benign	Left sphenoidal crest, rostral visual reflex	2
6	Female	50	Benign	Trigone of right ventricle, caudal visual reflex	7
7	Female	58	Benign	Left occipital lobe, caudal visual reflex	1.5
8	Male	48	Benign	Right sphenoidal crest, rostral visual reflex	2
9	Female	55	Benign	Left sphenoidal crest, rostral visual reflex	2
10	Male	54	Benign	Right frontoparietal area, lateral visual reflex	3
11	Male	54	Benign	Left temporal fossa, rostral visual reflex	2
12	Female	48	Benign	Tempus sinistrum, rostral visual reflex	2
13	Female	62	Benign	Left sphenoidal crest, rostral visual reflex	2
14	Male	55	Benign	Left sphenoidal crest, rostral visual reflex	3
15	Male	65	Benign	Left frontal lobe, rostral visual reflex	1.5
16	Male	57	Benign	Left temporal lobe, rostral visual reflex	5
17	Female	49	Benign	Right frontal lobe, rostral visual reflex	1.5
18	Male	47	Benign	Right frontal lobe, rostral visual reflex	1

Totally 18 patients completed the whole experiment. The patients were 10 males and 8 females, aged 46 to 65 years with a mean of 54.5 ± 6.12 years. The duration of disease was 1−7 years with an average of 2.72 ± 1.56 years. Clinical information of the 18 meningioma patients is presented in Table 1.

Conventional MRI, MR-DTI and radioactive tracing of meningioma patients
Conventional MRI results displayed tumor parenchyma, peritumoral edema and compression on surrounding brain tissue, the signal intensity was heterogeneous and the boundary was unclear. T2-weighted imaging signals were stronger and variable, while T1-weighted imaging signals were weaker and variable, and apparent reinforcement of tumor parenchyma was observed in enhanced scanning (Figures 1A−C). A three-dimensional visual radioactive tracing map for case 1 (Figure 1D) visualized the compression on the right lateral ventricle occipital horn, with moderate impairment or destruction, and the optic radiation on the affected side was observed to be thinner than that on the contralateral side.
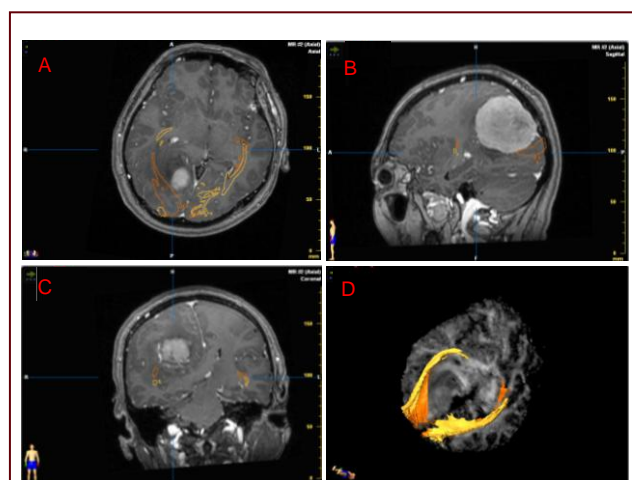

Figure 1   Three-dimensional radioactive tracing and conventional magnetic resonance imaging of optic-radiation fiber bundles in a parieto-occipital meningioma patient (case 1) before surgery using iPlan2.6 software.

The left lower part corresponds to the body position.

(A−C) Conventional magnetic resonance imaging of the compression on the tumor parenchyma, peritumoral edema and surrounding brain tissue.

White: Round parieto-occipital meningioma tumor; black: peritumoral edema; orange and yellow: superior and inferior bundles of optic-radiation fibers.

(D) Three-dimensional optic radiotrace showing the right lateral ventricle occipital horn compression, with moderate damage or destruction.

Yellow: Superior bundle of optic-radiation fibers; orange: inferior bundle of optic-radiation fibers.

DTI fractional anisotropy (FA) showed an unclear optic

radiation in the affected area. Green staining of the right Meyer's loop and a ventricle occipital triangular area weakened, and the optic radiation passing to the right ventricle occipital triangular area disappeared (white arrow) because of tumor compression, indicating the shift or destroying of the optic radiation. FA maps also visualized normal functional fiber bundles: the bilateral posterior limb of the internal capsule was stained blue because it consists of the corticospinal tract and cortical brainstem, while the right internal capsule transferred to the midline, but there was no significant difference in color. The normal corpus callosum was stained red at the knees and in the compressed area, showing normal function (Figure 2).
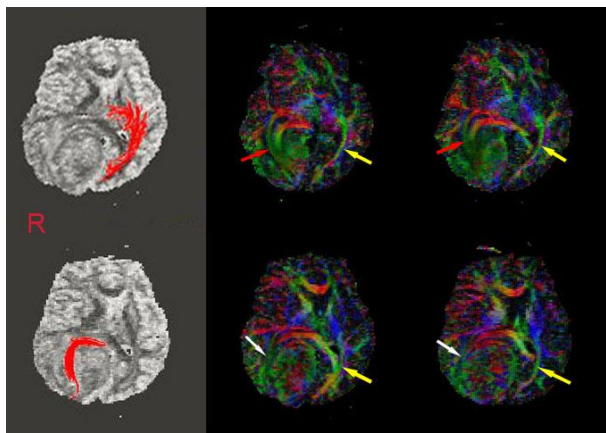

Figure 2   Optic radiation involving tissues in the parieto-occipital meningioma patient (case 1) observed by magnetic resonance-diffusion tensor imaging using diffusion tensor imaging-Studio software.

The left two images are fractional anisotropy images; red refers to the optic radiation beam traced by the diffusion tensor imaging-Studio software.

The right four images are color-coded tensor images; the bilateral internal capsule of the hind limb is blue, the right internal capsule transfers to the midline, and the normal corpus callosum is stained red.

The optic-radiation beam on the unaffected side shows normal morphology (yellow arrow), while the optic-radiation beam on the affected side is reduced (red arrow); white arrows indicate the absence of a radiation beam under tumor compression. R: Right.

The three-dimensional optic-radiation tracing map in case 2 visualized that the right lateral ventricle occipital horn transferred to the cerebral midline, with moderate impairment or destruction, and the optic-radiation beam was thinner than that on the unaffected side (Figure 3). The number of optic-radiation strips in patients traced by DTI using DTI-Studio software was significantly less than the number for the healthy side (Figure 4). FA maps showed that the green density of Meyer's loop at the right optic radiation disappeared, and that the occipital angle also notably reduced (Figure 4).
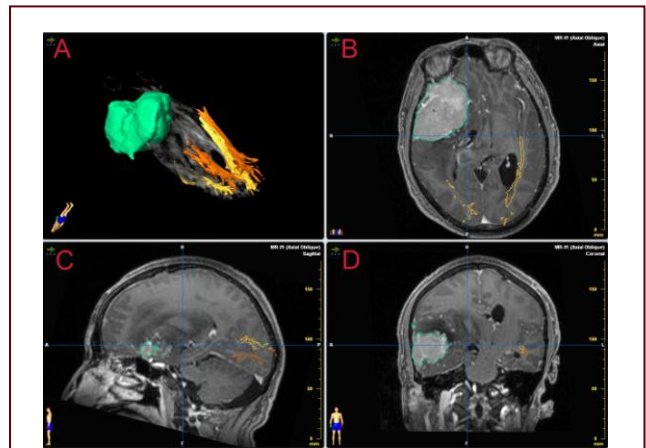

Figure 3   Preoperative three-dimensional tracing of optic-radiation fibers at the right sphenoid ridge meningioma patient (case 2) using iPlan2.6 software. The left lower part corresponds with the body position.

(A) Three-dimensional visual radiotrace showing the right lateral ventricle occipital horn under compression is close to the brain midline, with moderate impairment or destruction. Yellow: inferior bundle of optic-radiation fibers; orange: superior bundle of optic-radiation fibers.

(B–D) Conventional magnetic resonance imaging showing the tumor parenchyma, peritumoral edema and surrounding brain tissue, as well as optic-radiation fiber compression.

The white irregular round-like substance is a sphenoid ridge meningioma, the black substance around the tumor is a peritumoral edema, and orange and yellow respectively indicate the superior and inferior parts of optic-radiation fibers.
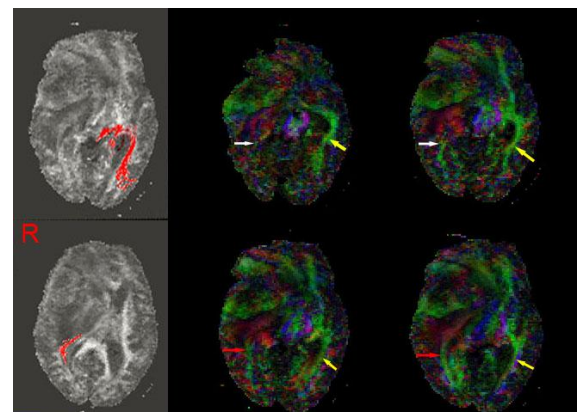

Figure 4   Fractional anisotropy and color-coded tensor diagram (diffusion tensor imaging-Studio software) for the right sphenoid ridge meningioma patient (case 2).

The red stain in the left two images indicates an optic-radiation bundle traced using diffusion tensor imaging-Studio software. Fractional anisotropy images show a significant decline in optic-radiation strips for the right optic-radiation Meyer's ring and ventricle occipital horn.

The contralateral optic-radiation bundle shows normal morphology (yellow arrow), while the optic-radiation beam on the affected side is reduced (red arrow). White arrows indicate the absence of an optic-radiation beam due to tumor compression. R: Right.

FA values

In the group of patients, there was one case of complete destruction of the optic radiation, with an FA value ratio of the affected side to the contralateral side of 10.5%; three cases of shift and moderate destruction, with FA value ratios of 46.3%, 40.5% and 37.4%; 11 cases of slight shifting, with the FA value ratio having a mean of 69.6%; and three normal or nearly normal cases, with an FA value ratio greater than 75%.

Correlation between the optic radiation and FA values

Patients were classified into four intervals of the ratio of the FA value for the affected side to that for the healthy side. Patients in the first interval, having a ratio less than 25%, had complete destruction of the optic radiation; patients in the second interval, having a ratio of 25−50%, had moderate damage; patients in the third interval, having a ratio of 50−75%, had a shifted optic radiation; and patients in the fourth interval, having a ratio greater than 75%, had a normal or nearly normal optic radiation. The results of conventional MRI, FA, color-coded tensor maps and three-dimensional white-matter tracing were compared. The FA value ratio for malignant meningioma patients was 10.5%, corresponding to the first interval, and FA images failed to show the optic-radiation beam, suggesting that white matter had been completely destroyed. The FA value in case 1 was 37.4%, corresponding to the second interval, and the color-coded tensor map and optic radiotrace showed an optic-radiation shift and partial defect (Figure 2). Cases corresponding to the third and fourth intervals only developed an optic-radiation shift or symmetry of the radiation shape, size, position and color.

DISCUSSION

Studies addressing the effect of MR-DTI on white-matter fibers in tumor patients have focused on tumor-relevant and surrounding indicators, such as the apparent diffusion coefficient, FA value and relative FA values, which are used to distinguish tumor parenchyma and peritumoral edema, as well as focusing on the role of these indicators in tumor classification[24-26]. Although there are still no generally accepted parameters or standards, the FA value is widely recognized as a meaningful indicator because it sensitively determines the degree of molecular diffusion in different directions, thus representing the changes in form and structure of white-matter fibers. Witwer *et al* [27] found that altered FA values in regions of interest corresponded with clinical manifestations in brain-tumor patients before and after surgery according to a DTI trace. Sinha *et al* [28] analyzed the correlation between FA values and white-matter changes in glioma patients, and showed that the change in the FA value can determine white-matter fiber tracts. In this study, the tumors are prone to alter the optic radiation, which was completely destroyed in one case, moderately damaged in one case, mildly damaged in six

cases, and shifted in eight cases, while it was unaffected in three cases owing to the optic radiation being too far away to affect the tumor-prone site. In this study, there were four cases of a meningioma at the caudal radiation, for which there were very strong T2WI optic-radiation signals. In one case, the optic-radiation image for white matter showed no significant change and the FA value ratio was 80%, while in the remaining three cases, there was old infarction at the occipital lobe and the FA values considerably decreased, which was in accordance with the fact that the necrotic neurons may develop retrograde Wallerian degeneration under the fiber bundle[29]. DTI is sensitive to the Wallerian degeneration of optic-radiation fibers after years of a compression meningioma leads to ischemic infarction at the occipital cortex and white matter. Fourteen cases with meningiomas located in the rostral and lateral optic radiations showed that the tumor developed a shift in the brain tissue according to conventional MRI, but this insult cannot affect white-matter fiber bundles. DTI clearly displayed the integrity of adjacent white-matter fiber bundles and the correlation between a meningioma and adjacent white-matter fiber bundles. Normal white-matter fibers provided strong signals in FA maps, which visualize the anatomical relationship between the tumor and surrounding white-matter fiber bundles, thus demonstrating a peritumoral white-matter fiber shift. This study found that, in benign meningioma patients, FA values remained the same in three cases that white-matter fibers were mildly compressed; however, the FA values for adjacent white matter were higher than those on the contralateral side under great compression. This is due to the compressed white-matter fiber being arranged more densely and a change in the fiber orientation; thus, there was greater alignment of fibers. The FA values decreased as a result of the adjacent brain tissue edema and the white-matter fiber signal weakened. A malignant meningioma is a kind of destructive lesion in the brain, and adjacent white-matter fiber bundles were obviously damaged, disrupted or not present, with visible infiltration or destruction; FA values were less; the signals at the edema were weaker; and FA values were less than in the case of a benign meningioma edema. The main reasons may be that (1) vasogenic edema activates the diffusion of water molecules in all directions, thus decreasing anisotropy and corresponding FA values, and (2) the number of water molecules within the extracellular space increased, thus decreasing the number of nerve fibers per unit volume, and there was less restriction on water molecule diffusion and lower anisotropy. Since there were only a few cases with malignant meningiomas, further studies are required to conclusively determine whether the change in FA value can reflect tumor pathological classification.

In summary, DTI is of importance to the treatment of large tumors and malignant meningiomas that are close to the optic radiation. Preoperative DTI information can

be used to evaluate visual protection, thus minimizing neurological impairment by employing an appropriate surgical approach and surgical procedures. At the same time, preoperative DTI reconstruction can be employed to introduce surgical risk to patients and their families. Therefore, we believe that DTI visualizes important conduction bundles, thus assisting preoperative assessment. Previous work by our research group has confirmed the feasibility, accuracy and authenticity of the tracer reconstruction of optic-radiation fibers. The course of the reconstructed optic radiation well matches classical anatomical theory.

SUBJECTS AND METHODS

Design
A clinical radiological observation.

Time and setting
Experiments were performed from December 2010 to August 2011 in the Nuclear Magnetic Resonance Laboratory, Department of Neurosurgery Surgery, Chinese PLA General Hospital, China.

Subjects
Totally 18 patients with a meningioma close to optic-radiation lesions were examined by MRI at the Chinese PLA General Hospital from June 2010 to June 2011. The patients were 10 males and eight females, aged 46–65 years. Cases of congenital blindness, unilateral blindness, post-traumatic optic atrophy and bilateral meningioma were excluded. All patients were confirmed by pathology and pathologically classified as being of fiber type in five cases, epithelial type in four cases, transitional type in four cases, hemangioma in three cases, atypical type in one case, mixed type in one case, and anaplastic (malignant) in one case. The location of the meningioma was the supratentorial brain convexity in five cases, cerebral falx in three cases, superior sagittal sinus in two cases, sphenoidal crest in six cases, and lateral ventricle trigone in two cases. All patients and their families were informed of the purpose and necessity of MRI examination prior to the experiment, and the experimental disposals were in line with the Declaration of Helsinki.

Methods

MRI scans
All MRI scans were performed with a scanner incorporating a 1.5-T magnet (Siemens Espree, Erlangen, Germany). The sequence parameters were as follows. DTI: Single-shot spin-echo diffusion-weighted echo-planar imaging sequence. Sequence parameters of TE 147 ms, TR 9 400 ms, matrix 128 × 128, FOV 251 × 251 mm, slice thickness 3 mm, bandwidth 1 502 Hz/px. Diffusion weights (high b value) 1 000 s/mm^2, 12 directions of diffusion-weighted imaging, simultaneous 0-diffusion-weighted imaging (b0, low b value 0 s/mm^2) to eliminate post-peripheral noise. Voxel size 1.9 mm × 1.9 mm × 3 mm. Forty layers continuously acquired a total of five times to improve the signal-to-noise ratio.

T1WI: T1-weighted three-dimensional magnetization-prepared rapid gradient-echo imaging sequence. Parameters including TE 3.02 ms, TR 1 650 ms, matrix 256 × 256, FOV 250 × 250 mm, slice thickness 1 mm, slab thickness 1 mm) were designated to build anatomical images.
T2WI: TE 93 ms, TR 5 500 ms, matrix 512 × 512, FOV 230 × 230 mm, slice thickness 3 mm.
T2flair: TE 84 ms, TR 9 000 ms, matrix 256 × 256, FOV 230 × 230 mm, slice thickness 3 mm.
All collected data were transferred through a local area network to workstations on which the navigation program was used. The data format was converted using PatXfer 5.2 software (BrainLab, Feldkirchen, Germany), and conventional MRI images were obtained with iPlan 2.6 software (BrainLab). The lesions were outlined and optic-radiation fiber bundles were three-dimensionally traced. DTI-Studio software (CMRM at Johns Hopkins Medical Institute, Baltimore, MD, USA) was applied to plot color-coded tensor images and to measure the FA values for the affected and healthy sides.

Three-dimensional tracing of optic-radiation fibers
Three-dimensional tracing was carried out employing linear expansion based on the tensor deviation algorithm[30]. The direction of the maximal vector axis at the adjacent voxel served as the orientation of the optic radiation in reconstruction. The "fiber tracking" module of the neuronavigation program software iPlan 2.6 was used for the tracing of the optic radiation. The threshold of the FA was defined as 0.15 and the minimum fiber length was 50 mm (termination condition). The optic radiation was reconstructed in the fused T1 anatomical image employing multi-volume of interest methods to reconstruct Meyer's loop. The first region of interest was located in the lateral geniculate body, and the second region of interest in the occipital calcarine lower-lip cleft cortex. When we reconstructed the dorsal beam (central beam and posterior beam), the first region of interest was located in the lateral geniculate body, and the second region of interest in the occipital calcarine split-upper-lip cortex. In the axial view, the cerebral peduncle and posterior limb internal capsule simultaneously crossing through the optic-radiation fibers in the two regions of interest is considered the optic radiation. The "create" function of iPlan 2.6 can be used to connect the peripheral closed curve of the optic radiation in each layer, thus displaying the three-dimensional optic radiation.

Bilateral optic-radiation FA values
DTI-Studio software was used to measure optic-radiation FA values[31]. According to nerve anatomy histology[32-34], regions of interest of the optic radiation were selected from the lateral ventricle trigone and used to measure bilateral optic-radiation FA values.

REFERENCES

[1] Peltier J, Travers N, Destrieux C, et al. Optic radiations: a microsurgical anatomical study. J Neurosurg. 2006;105(2):294-300.

[2] Coppens JR, Mahaney KB, Abdulrauf SI. An anteromedial approach to the temporal horn to avoid injury to the optic radiation fibers and uncinate fasciculus: anatomical and technical note. Neurosurg Focus. 2005;18(6B):E3.

[3] Sincoff EH, Tan Y, Abdulrauf SI. White matter fiber dissection of the optic radiations of the temporal lobe and implications for surgical approaches to the temporal horn. J Neurosurg. 2004;101(5):739-746.

[4] Rubino PA, Rhoton AL Jr, Tong X, et al. Three-dimensional relationships of the optic radiation. Neurosurgery. 2005;57(4 Suppl):219-227.

[5] Peuskens D, van Loon J, Van Calenbergh F, et al. Anatomy of the anterior temporal lobe and the frontotemporal region demonstrated by fiber dissection. Neurosurgery. 2004;55(5):1174-1184.

[6] Kovanlikaya I, Firat Z, Kovanlikaya A, et al. Assessment of the corticospinal tract alterations before and after resection of brainstem lesions using Diffusion Tensor Imaging (DTI) and tractography at 3T. Eur J Radiol. 2011;77(3):383-391.

[7] Nelles M, Gieseke J, Flacke S, et al. Diffusion tensor pyramidal tractography in patients with anterior choroidal artery infarcts. AJNR Am J Neuroradiol. 2008;29(3):488-493.

[8] Nilsson C, Markenroth Bloch K, Brockstedt S, et al. Tracking the neurodegeneration of parkinsonian disorders--a pilot study. Neuroradiology. 2007;49(2):111-119.

[9] Yasmin H, Nakata Y, Aoki S, et al. Diffusion abnormalities of the uncinate fasciculus in Alzheimer's disease: diffusion tensor tract-specific analysis using a new method to measure the core of the tract. Neuroradiology. 2008;50(4):293-299.

[10] Kvickström P, Eriksson B, van Westen D, et al. Selective frontal neurodegeneration of the inferior fronto-occipital fasciculus in progressive supranuclear palsy (PSP) demonstrated by diffusion tensor tractography. BMC Neurol. 2011;11:13.

[11] Trivedi R, Anuradha H, Agarwal A, et al. Correlation of quantitative diffusion tensor tractography with clinical grades of subacute sclerosing panencephalitis. AJNR Am J Neuroradiol. 2011;32(4):714-720.

[12] Hong JH, Son SM, Jang SH. Somatotopic location of corticospinal tract at pons in human brain: a diffusion tensor tractography study. Neuroimage. 2010;51(3):952-955.

[13] Hong JH, Jang SH. The usefulness of DTI for estimating the state of cerebellar peduncles in cerebral infarct. NeuroRehabilitation. 2010;26(4):299-305.

[14] Kamali A, Kramer LA, Butler IJ, et al. Diffusion tensor tractography of the somatosensory system in the human brainstem: initial findings using high isotropic spatial resolution at 3.0 T. Eur Radiol. 2009;19(6):1480-1488.

[15] Klose U, Mader I, Unrath A, et al. Directional correlation in white matter tracks of the human brain. J Magn Reson Imaging. 2004;20(1):25-30.

[16] Stieglitz LH, Lüdemann WO, Giordano M, et al. Optic radiation fiber tracking using anteriorly angulated diffusion tensor imaging: a tested algorithm for quick application. Neurosurgery. 2011;68(5):1239-1251.

[17] Polonara G, Salvolini S, Fabri M, et al. Unilateral visual loss due to ischaemic injury in the right calcarine region: a functional magnetic resonance imaging and diffusion tension imaging follow-up study. Int Ophthalmol. 2011;31(2):129-134.

[18] Engelhorn T, Michelson G, Waerntges S, et al. Diffusion tensor imaging detects rarefaction of optic radiation in glaucoma patients. Acad Radiol. 2011;18(6):764-769.

[19] Tao XF, Wang ZQ, Gong WQ, et al. A new study on diffusion tensor imaging of the whole visual pathway fiber bundle and clinical application. Chin Med J (Engl). 2009;122(2):178-182.

[20] Sherbondy AJ, Dougherty RF, Napel S, et al. Identifying the human optic radiation using diffusion imaging and fiber tractography. J Vis. 2008;8(10):12.1-11.

[21] Xie S, Gong GL, Xiao JX, et al. Underdevelopment of optic radiation in children with amblyopia: a tractography study. Am J Ophthalmol. 2007;143(4):642-646.

[22] Lehéricy S, Duffau H, Cornu P, et al. Correspondence between functional magnetic resonance imaging somatotopy and individual brain anatomy of the central region: comparison with intraoperative stimulation in patients with brain tumors. J Neurosurg. 2000;92(4):589-598.

[23] Bittar RG, Olivier A, Sadikot AF, et al. Cortical motor and somatosensory representation: effect of cerebral lesions. J Neurosurg. 2000;92(2):242-248.

[24] Brunberg JA, Chenevert TL, McKeever PE, et al. In vivo MR determination of water diffusion coefficients and diffusion anisotropy: correlation with structural alteration in gliomas of the cerebral hemispheres. AJNR Am J Neuroradiol. 1995;16(2):361-371.

[25] Holodny AI, Ollenschlager M. Diffusion imaging in brain tumors. Neuroimaging Clin N Am. 2002;12(1):107-124,x.

[26] Le Bihan D, Mangin JF, Poupon C, et al. Diffusion tensor imaging: concepts and applications. J Magn Reson Imaging. 2001;13(4):534-546.

[27] Witwer BP, Moftakhar R, Hasan KM, et al. Diffusion-tensor imaging of white matter tracts in patients with cerebral neoplasm. J Neurosurg. 2002;97(3):568-575.

[28] Sinha S, Bastin ME, Whittle IR, et al. Diffusion tensor MR imaging of high-grade cerebral gliomas. AJNR Am J Neuroradiol. 2002;23(4):520-527.

[29] Serrano-Pozo A, González-Marcos JR, Castell-Monsalve J. Wallerian degeneration of the corticospinal tract following spontaneous brain haematoma. Rev Neurol. 2005;41(8):501-502.

[30] Chen X, Weigel D, Ganslandt O, et al. Prediction of visual field deficits by diffusion tensor imaging in temporal lobe epilepsy surgery. Neuroimage. 2009;45(2):286-297.

[31] Jiang H, van Zijl PC, Kim J, et al. DtiStudio: resource program for diffusion tensor computation and fiber bundle tracking. Comput Methods Programs Biomed. 2006;81(2):106-116.

[32] Bürgel U, Mecklenburg I, Blohm U, et al. Histological visualization of long fiber tracts in the white matter of adult human brains. J Hirnforsch. 1997;38(3):397-404.

[33] Rademacher J, Bürgel U, Geyer S, et al. Variability and asymmetry in the human precentral motor system. A cytoarchitectonic and myeloarchitectonic brain mapping study. Brain. 2001;124(Pt 11):2232-2258.

[34] Yu CS, Li KC, Xuan Y, et al. Diffusion tensor tractography in patients with cerebral tumors: a helpful technique for neurosurgical planning and postoperative assessment. Eur J Radiol. 2005;56(2):197-204.

(Edited by Liu M, Chen B/Yang Y/Song LP)